

International Journal of Modern Physics A  
 © World Scientific Publishing Company

## DYNAMICAL EVOLUTION OF CLUSTERS OF GALAXIES: THE EFFECT OF HIGH-VELOCITY SUBSTRUCTURE CLUMPS

A. DEL POPOLO

*Dipartimento di Matematica, Università Statale di Bergamo, Piazza Rosate 2 - I 24129  
 Bergamo, ITALY*

*Feza Gürsey Institute, P.O. Box 6 Çengelköy, İstanbul, Turkey*

*Boğaziçi University, Physics Department, 80815 Bebek, İstanbul, Turkey*

M. GAMBERA

*Dipartimento di Matematica, Università Statale di Bergamo, Piazza Rosate 2 - I 24129  
 Bergamo, ITALY*

E. NIHAL ERCAN

*Boğaziçi University, Physics Department, 80815 Bebek, İstanbul, Turkey*

Received (Day Month Year)

Revised (Day Month Year)

In the Cold Dark Matter (hereafter CDM) scenario even isolated density peaks contain a high fraction of small scale clumps having velocities larger than the average escape velocity from the structure. These clumps populate protoclusters, especially in the peripheral regions,  $r \geq R_f$  (where  $R_f$  is the filtering scale). During the cluster collapse and the subsequent secondary infall, collapsing or infalling clumps (having  $v < v_{\text{esc}}$ ) interact with the quoted *unbound* clumps (or *high speed clumps*, as we also call them) having  $v > v_{\text{esc}}$ . We study the interaction between these two kind of clumps by means of the impulse approximation<sup>1</sup> and we find that the collapse of *bound* clumps is accelerated with respect to the homogeneous case (Gunn & Gott's model, Ref. 2). The acceleration of the collapse increases with decreasing height of the peak,  $\nu$ . We finally compare the acceleration produced by this effect to the slowing down effect produced by the gravitational interaction of the quadrupole moment of the system with the tidal field of the matter of the neighboring proto-clusters studied in Del Popolo & Gambera<sup>3</sup>. We find that the magnitude of the slowing down effect is larger than the acceleration produced by the effect studied in this paper, only in the outskirts of the cluster. We want to stress that the one which we study in this paper is also present in an isolated protocluster, being produced by the interaction of the collapsing clumps with the *unbound* substructure internal to the collapsing clumps itself while that studied in Ref. 3 is produced by substructure external to the density peak.

*Keywords:* cosmology: theory-large scale structure of Universe - galaxies: formation.

## 1. Introduction

According to the most promising cosmological scenarios, structure formation is traced back to the evolution of primordial density fluctuations. These fluctuations, originated from quantum fluctuations<sup>4,5,6,7</sup> in an inflationary phase of the early Universe, grew up through gravitational instability to a maximum radius  $r_m$ . At the time  $t_m$  corresponding to maximum expansion, perturbations broke away from the general expansion and at  $\bar{\delta} \sim 1$  they began to collapse. Hence the collapse of perturbations onto local density maxima of the primordial density field has a key role in structure formation and several studies deal with this problem. The problem of collapse has been investigated from two points of view, namely:

- i) that of the statistical distribution of the objects formed<sup>7,8</sup>
- ii) that of the structure of these objects and its dependence on the statistical properties of the primordial density field<sup>2,9,10,11,12,13,14,15,16,17,18,19,20,21,22,23,24</sup>.

In the spherical accretion model introduced by Hoyle and Narlikar<sup>25</sup> and applied to clusters of galaxies by Gunn & Gott<sup>2</sup>, the matter around the core of the perturbation is a homogeneous fluid with zero pressure. If the density inside the perturbation is greater than the critical density, it is bound and shall expand to a maximum radius  $r_m$ :

$$r_m = \frac{r_i}{\bar{\delta}} \quad (1)$$

where  $r_i$  is the initial radius and  $\bar{\delta}$  is the overdensity inside the radius  $r$ . Such matter shall collapse in a time

$$T_{c0}/2 = \frac{\pi}{H_i} \frac{(1 + \bar{\delta})}{\bar{\delta}^{3/2}} \quad (2)$$

where  $H_i$  is the Hubble parameter at the initial time  $t_i$ .

This model was introduced in order to overcome the problem of the excessively steep density profiles,  $\rho \propto r^{-4}$ , obtained in numerical experiments of simple gravitational collapse. Some authors were able to produce shallower profiles<sup>2,26,27</sup>,  $\rho \propto r^{-2}$ , through the *secondary infall* process. Several years later, observational evidences for secondary infall in the outskirts of clusters of galaxies has been reported in Ref. 28, 29.

Even if this model and in general the original form of SIM (secondary infall model) is able to explain better than previous models the structure of clusters of galaxies it has some drawbacks, (e.g. it does not predict the right structure of density profiles), that can be overcome with some improvements in the original model<sup>30</sup>. Two noteworthy limits by the Gunn & Gott<sup>2</sup> model are the following:

- a) It neglects tidal interaction of the perturbation with the neighboring perturbation;

b) It neglects substructure existing in the outskirts of proto-galaxies or proto-clusters and in the background.

The effect of the tidal field was studied in a recent paper<sup>3</sup>. In that paper, we showed that the gravitational interaction of the quadrupole momentum of a proto-structure with the tidal field of the neighboring proto-structures introduces another potential energy term in the equation describing the collapse which acts in the sense to delay the collapse. This effect has revealed as one of noteworthy importance in solving several of the drawbacks of the CDM model<sup>3,31,32,33</sup>, namely:

- 1) lack of a mechanism originating the bias<sup>3</sup>;
- 2) discrepancies between:
  - a1) X-ray temperature function of clusters and observations<sup>31</sup>.
  - a2) two-point correlation function of clusters and observations<sup>31</sup>;
  - a3) mass function and velocity dispersion function of clusters and observations<sup>33</sup>;
  - a4) shape of clusters and observations<sup>34</sup>;
  - a5) angular two-point correlation function of galaxies and observations<sup>32</sup>.

For what concerns point "b)", we may say that during the last two decades, astronomers have discovered that at least a third of galaxy clusters are not dynamically relaxed systems but contain substructure on scales of the same order as the cluster itself<sup>34,35,36</sup>. This implies that clusters are currently forming or have formed recently enough that they have not had time to undergo significant degree of violent relaxation and phase mixing. When one studies the structure of the velocity field around a peak one finds that at radii  $r$  larger than the filtering scale  $R_f$ , ( $r \geq R_f$ ), a sensitive fraction of the matter of the peak is gravitationally unbound to it<sup>37</sup>. This is not surprising since a non zero fraction of unbound matter should be expected even in the case of a uniform system with a Maxwellian velocity distribution (see section 2.2 for a discussion).

The encounters between collapsing clumps and the unbound high velocity clumps influence the collapse of the proto-cluster. We want to study this point and to compare its effect on cluster collapse with that produced by the effects of tidal interaction of the protocluster with the neighboring ones.

In the following we show how the unbound substructures influences the collapse of the perturbation. The plan of this work is the following: in Section 2 we deal with the unbound substructure effects. In Section 3 we give our results and finally Section 4 is devoted to the conclusions.

## 2. Unbound substructure effects

Our cosmological setting is described by a hierarchical clustering scenario, a CDM model (see Ref. 38) in which structure formation goes *bottom-up*. Local density extrema are assumed to be the sites of structure formation<sup>7,8</sup>. The perturbations

grows linearly until the linearly evolved dispersion  $\sigma(z, M)$  of the density contrast is  $< 1$ , while it enters in the non-linear phase when  $\sigma(z, M) = 1$ . Denoting this epoch by  $z_{\text{nl}}$  one has:

$$\sigma_0(M) = 1 + z_{\text{nl}} \quad (3)$$

(Liddle & Lyth<sup>38</sup>, equation 8.2), where as always the subscript 0 denotes the present value of the linearly evolved quantity and  $\sigma_0(M)$  is related to the power spectrum  $P(k)$  of density fluctuations by:

$$\sigma_0(M) = \frac{1}{2\pi^2} \int P(k) k^2 W(kR_f) dk \quad (4)$$

being  $R_f$  the filtering scale and  $W(kR_f)$  the window function:

$$W(kR_f) = \frac{3[\sin(kR_f) - kR_f \cos(kR_f)]}{(kR_f)^3} \quad (5)$$

A subgalactic mass scale collapses at a redshift:

$$1 + z_{\text{nl}} = \frac{30}{b} \quad (6)$$

(Silk & Stebbins<sup>39</sup>), where  $b$  is the biasing parameter. In particular a perturbation of  $10^{15} M_\odot$  collapses at a redshift  $z \simeq 0.02$  while perturbations in the range  $10^6 M_\odot \div 10^9 M_\odot$  collapse almost at the same  $z \simeq 18$  because the mass variance in this region varies only of a factor 3 (Ref. 40). A part of this last perturbations have a cross section too little for gravitational merging to be destroyed<sup>40</sup>. Therefore a mass perturbation  $> 10^8 M_\odot$  (see Ref. 38) can survive until the cluster enters non-linear phase at  $z \simeq 0.02$ .

In order to study the dynamical evolution of the proto-cluster, we use the shell method<sup>3,41,42,43</sup>. If we consider a shell of matter around the centre of the cluster this is made of galaxies, gas and substructure. During the collapse, the shell encounters clouds of substructure some of which have high speed. Supposing that the systems subject to the encounter (the shell of matter and the high speed clumps) have, respectively, median radii  $r_1$  and  $r_2$ , velocity dispersions of order  $\sigma_1, \sigma_2$ , that at the instant of closest approach their centres are separated by  $b'$  and have relative speed  $V$  the condition<sup>44</sup>:

$$V \gg \sigma_i \frac{\max(r_1, r_2, b')}{r_i} \quad i = 1, 2 \quad (7)$$

ensures that in the course of the encounter the objects constituting the encountering systems barely move from their initial locations. The result of the encounter is to generate perturbations in the velocity and energy of the objects constituting the shell (here we are only interested in the effect of the encounter on the shell). In fact the effects of high speed encounters on the internal structure of "stellar" systems decrease as the encounter speed increases and consequently high speed encounters generate only small perturbations of otherwise steady-state systems.

The conditions expressed in equation (7) is known as impulse approximation (hereafter IA)<sup>1</sup> and yields accurate results often even when the condition is not strictly satisfied. As stressed by Gnedin & Ostriker<sup>42</sup>, the IA works well in the outer region of clusters, wherein galaxies are assumed to move little during the interaction, while the IA is not appropriate in the cluster core.

### 2.1. Applicability of the IA

Before going on, we want to analyze the applicability of the IA as expressed by equation (7) to our problem.

A first rough analysis can be performed remembering that the escape velocity in the cluster is fixed by the virial theorem according to equation (see for example Ref. 44, (equation (8.3))):

$$\langle v_{\text{esc}}^2 \rangle = 4 \langle v^2 \rangle \quad (8)$$

where  $v_{\text{esc}}$  is the escape velocity and  $\langle v^2 \rangle$  is the 3-D dispersion velocity, and

$$\langle v^2 \rangle = 3\sigma_1^2 \quad (9)$$

being  $\sigma_1$  the velocity dispersion of the objects constituting the shell, and then

$$v_{\text{esc}} = \sqrt{12}\sigma_1 \quad (10)$$

The relative velocity,  $V$ , is the sum of the infall velocity of the shell and the velocity of clumps moving outwards:

$$V \simeq v_{\text{clumps}} + v_{\text{infalling shell}} \quad (11)$$

Imposing that the clumps move at speed larger than  $v_{\text{esc}}$ , we get:

$$v_{\text{clumps}} > v_{\text{esc}} = \sqrt{12}\sigma_1 = 2\sqrt{3}\sigma_1 \quad (12)$$

The infalling shells are marginally bound, hence they travel at a velocity close to the local escape velocity

$$v_{\text{infalling shell}} \leq v_{\text{esc}} = \sqrt{12}\sigma_1 \quad (13)$$

This last statement can be easily proven using for example an Hernquist model for the cluster. In general, conservation of energy yields:

$$v_{\text{infalling shell}}^2 = v_{\text{esc}}^2 + 2\Phi(r_a), \quad (14)$$

where  $\Phi$  is the (negative) potential and  $r_a$  is the maximum (apocentric) radius of the infalling particle.

For example, for a Hernquist cluster, one has

$$\Phi(r) = -GM/(r + a) \quad (15)$$

and

$$v_{\text{infalling shell}}^2(r) = 2[\Phi(r_a) - \Phi(r)] = v_{\text{esc}}^2(r)[1 - (r+a)/(r_a+a)] = v_{\text{esc}}^2(r)(r_a - r)/(r_a + a) \quad (16)$$

For a Hernquist model,  $a$  is a few tenths of the virial radius. The infalling particles are between the virial and turnaround radii, i.e. between  $r_{\text{vir}}$  and roughly  $2 r_{\text{vir}}$ . So  $r_a \gg a$  and

$$v_{\text{infalling shell}}^2(r) = v_{\text{esc}}^2(r)(1 - r/r_a) \quad (17)$$

which means that  $v_{\text{infalling shell}}$  is a little smaller than  $v_{\text{esc}}$ .

Using the previous results (equation (12) and (13)), we have:

$$V \simeq v_{\text{clumps}} + v_{\text{infalling shell}} = 2\sqrt{3}\sigma_1 + \sqrt{12}\sigma_1 \simeq 7\sigma_1 \quad (18)$$

If  $i = 1$ , in Eq. (7), we are dealing with the shell then:

1)  $V = 7\sigma_1 > \sigma_1$

If  $i = 2$ , we are dealing with the clump:  $\sigma_2 \simeq 1 \text{ km/s} \ll \sigma_1$  (see Ref. 39) and then:

2)  $V = 7\sigma_1 \gg \sigma_2$ .

Both the relations 1) and 2) satisfy the condition:

$$V \geq 7\sigma_1 \quad (19)$$

value that according to Ref. 44 (see page 440) is considered good to use the IA. We want to remark that the previous analysis does not take account of the reduction of escape velocity with radius: given the potential of the system,  $\Phi(r)$ , the escape velocity is  $v_{\text{esc}} = \sqrt{2|\Phi(r)|}$ . This means that going outwards the IA is more strictly satisfied.

## 2.2. Energy change in the shell

The energy change in the shell, due to an encounter with high velocity clumps, can be computed as follows.

Suppose to have a perturber (a high speed clump of substructure, member of the cluster) characterized by a speed larger than the escape speed from the cluster. This high velocity clump, that we stress is inside and part of the cluster, moves away from it. We use cylindrical coordinates  $(R, z)$  such that the  $z$ -axis coincides with the perturber's trajectory given by:

$$R = 0, \quad z = A(t) = Vt \quad (20)$$

and that  $R = 0, z = 0$  is the centre of the perturbed system (shell of matter). Note that we are interested only in clumps not contained in the core and moving from the centre in the outward direction, so that they do not go through the cluster centre. The choice of not taking into account the effect of clumps in the core area is due to Gnedin & Ostriker<sup>42</sup> observation that the IA works well in the outer region of clusters, wherein galaxies are assumed to move little during the interaction. The velocity increment  $\Delta v$  of a test particle at the position  $(R, z)$  is given by:

$$\Delta v_R = \int_0^\infty \frac{d\Phi}{dr} \frac{R}{r} dt = -\frac{R}{V} \int_0^\infty \frac{d\Phi}{dr} \frac{dA}{r} \quad (21)$$

where

$$r = [(A - z)^2 + R^2]^{1/2} \quad (22)$$

and  $\Phi$  is the potential of the perturber. Assuming that the perturber is an isothermal sphere it can be easily shown that:

$$\Delta v_R = -\pi \sigma_2^2 / V \quad (23)$$

where  $\sigma_2$  is the perturber internal velocity dispersion.

The energy, gained by the shell of matter during the encounter with a high velocity clump, is given by:

$$\Delta E = \int_0^\infty [\Delta v(R)]^2 \Sigma(R) R dR \quad (24)$$

(see Ref. 44) where  $\Sigma(R)$  is the surface density of the perturbed system.

We assume that the perturbed system (shell) is characterized by an average density given by:

$$\bar{\rho}(r_i, t) = \frac{3M}{4\pi a^3(r_i, t) r_i^3} \quad (25)$$

where, according to Ref. 2 notation,  $a(r_i, t)$  is the expansion factor of the shell at time  $t$ ,  $r_i$  its initial radius and  $M$  its mass. We are studying the collapse of a shell of matter then  $t_i$  and  $r_i$  coincide with the turn-around epoch and radius of the shell, respectively. Assuming that no shell crossing occurs, the total mass inside each shell stays constant and then:

$$\bar{\rho}(r_i, t) = \frac{\bar{\rho}(r_i, t_i)}{a^3(r_i, t)} \quad (26)$$

The surface density is given by:

$$\Sigma = \frac{\Sigma_i}{a(r_i, t)^2} \quad (27)$$

At this point we are ready to calculate the energy change in the shell by using equations (23), (24), (27) and remembering that  $r = r_i a(r_i, t)$ :

$$\Delta E = \pi^2 \frac{\sigma_2^4}{V^2} \Sigma_i r_i^2 (\log a_{\max} - \log a_{\min}) \quad (28)$$

where  $a_{\max}$  is the maximum value of the expansion parameter, corresponding to the turn-around epoch, and  $a_{\min}$  the minimum value of the expansion parameter corresponding to the time of full collapse of the perturbation. During infall a shell of matter experiences several encounters with all the unbound clumps located between its initial position and the final one. Each one of the encounters produces an increase of the energy of the shell. In order to calculate the total energy,  $\Delta E_T$ , acquired during infall we must calculate the number of unbound clumps "internal" to its orbit. The number of perturbers can be calculated observing that:

- aa) they are peaks of the density field having dimension much less than that of the cluster but large enough to survive till the cluster enters the non-linear phase;
- bb) they must satisfy the IA condition.

Clumps in the SCDM scenario are not distributed randomly but are clustered and so tend to be more bound to their nearby neighbors. This may make them more subject to mergers in some cases soon after they form, but may also prevent mergers by placing them in a high velocity dispersion environment. For survival, we must require a large density contrast to have developed. If the smaller scale fluctuations have a density contrast of  $\simeq 100$ , they should be able to survive tidal disruption or dynamical friction drag when its environment undergoes non-linear collapse. This translates into a minimum mass scale of  $\simeq 10^8 M_\odot$  (see Ref. 39). In order to determine the number density and the characteristics of these peaks we follow the same choice made by Antonuccio-Delogu & Colafrancesco<sup>44</sup> and Del Popolo & Gambera<sup>43</sup>. We restrict ourselves to consider a subset of peaks of the density field, having the central height  $\nu$  larger than a threshold  $\nu_c$ . The threshold is chosen by satisfying the condition its radius  $r_{\text{pk}}$  is smaller than the average peak separation,  $d_{\text{av}} = n_a^{-1/3}(\nu \geq \nu_c)$ :

$$r_{\text{pk}}(\nu \geq \nu_c) \leq 0.1 \cdot n_a^{-1/3}(\nu \geq \nu_c) \quad (29)$$

where the radius of a peak  $r_{\text{pk}}$  is given by:

$$r_{\text{pk}} = \sqrt{2}R_* \left[ \frac{1}{1 + \nu\sigma_0} \cdot \frac{1}{\gamma^3 + (0.9\nu)^{1.5}} \right]^{\frac{1}{3}} \quad (30)$$

(see Ref. 45), where:

$$\gamma = \sigma_1^2 / \sigma_0\sigma_2 \quad (31)$$

and here  $\sigma_i$  is the  $i$ -th momentum of the variance of the fluctuation field:

$$\sigma_i^2 = \frac{1}{2\pi^2} \int P(k)k^{2(i+1)}dk \quad (32)$$

where  $P(k)$  is the filtered power spectrum. The power spectrum that we adopt is  $P(k) = AkT^2(k)$  with the transfer function  $T(k)$  given in Ref. 7 (equation (G3)):

$$T(k) = \frac{[\ln(1 + 2.34q)]}{2.34q} \cdot [1 + 3.89q + (16.1q)^2 + (5.46q)^3 + (6.71)^4]^{-1/4} \quad (33)$$

where  $A$  is the normalizing constant and  $q = \frac{k\theta^{1/2}}{\Omega_X h^2 \text{Mpc}^{-1}}$ . Here  $\theta = \rho_{\text{er}}/(1.68\rho_\gamma)$  represents the ratio of the energy density in relativistic particles to that in photons ( $\theta = 1$  corresponds to photons and three flavors of relativistic neutrinos). For the previous CDM transfer function, normalized as  $\sigma_8 = 0.63$  and filtering radius  $R_f = 30 \text{Kpc}$ , (corresponding to a Gaussian filtered mass  $M \simeq 10^8 M_\odot$ ) one has  $\gamma = 0.48$ ,  $R_* = \sqrt{3\frac{\sigma_1}{\sigma_2}} = 33 \text{Kpc}$  and then  $\nu_c = 1.6$ . Remembering that the number

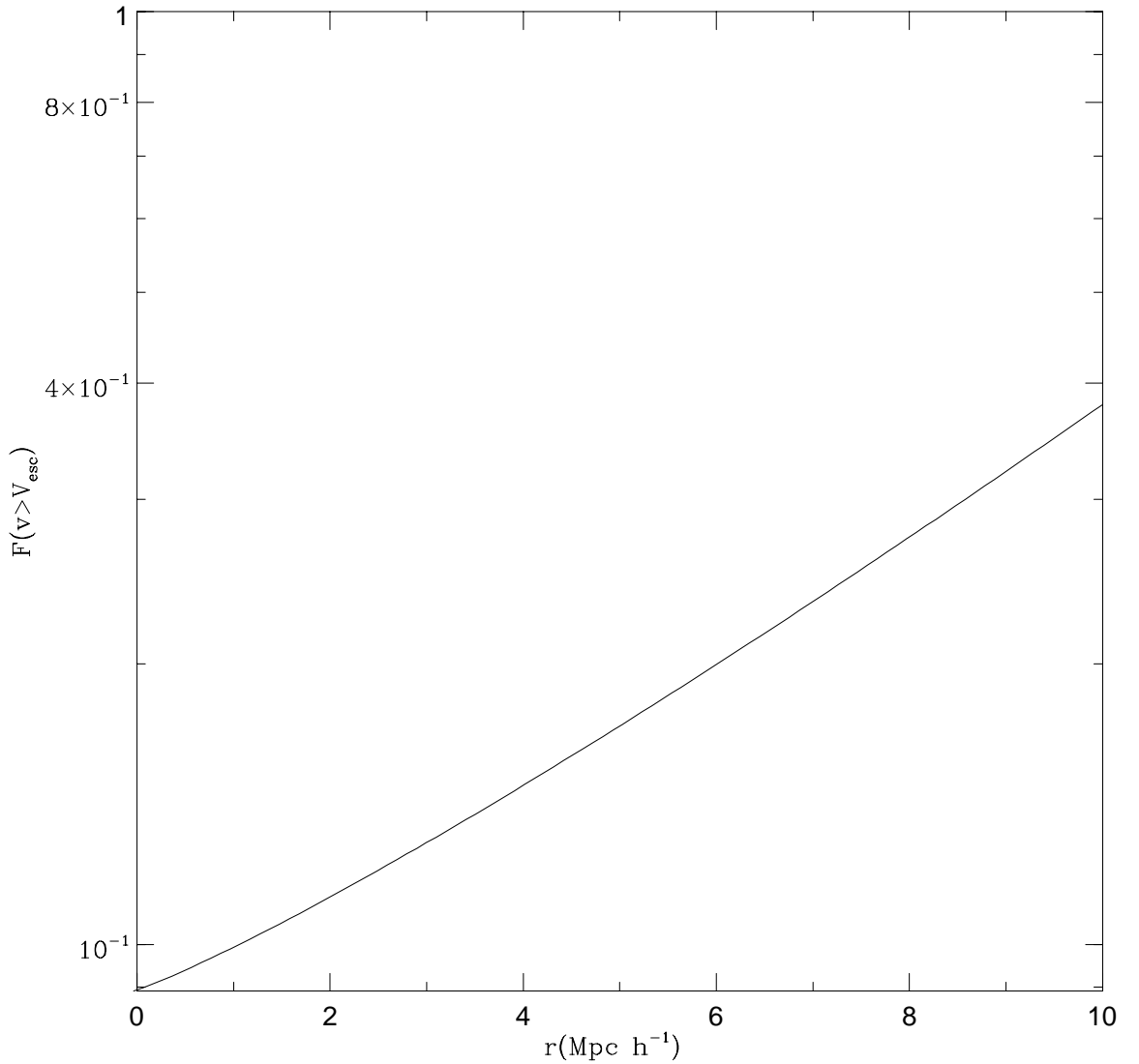


Fig. 1. Spatial variation of  $F(v \geq v_{\text{esc}})$  for the CDM spectrum, introduced in Section 2, smoothed on a scale  $R_f = 5h^{-1}$  Mpc and for  $\nu = 1.2$ .

density of peaks,  $n_a$ , having  $\nu \geq \nu_c$ , is given by:

$$n_a = \int_{\nu_c}^{\infty} N_{\text{pk}} d\nu \quad (34)$$

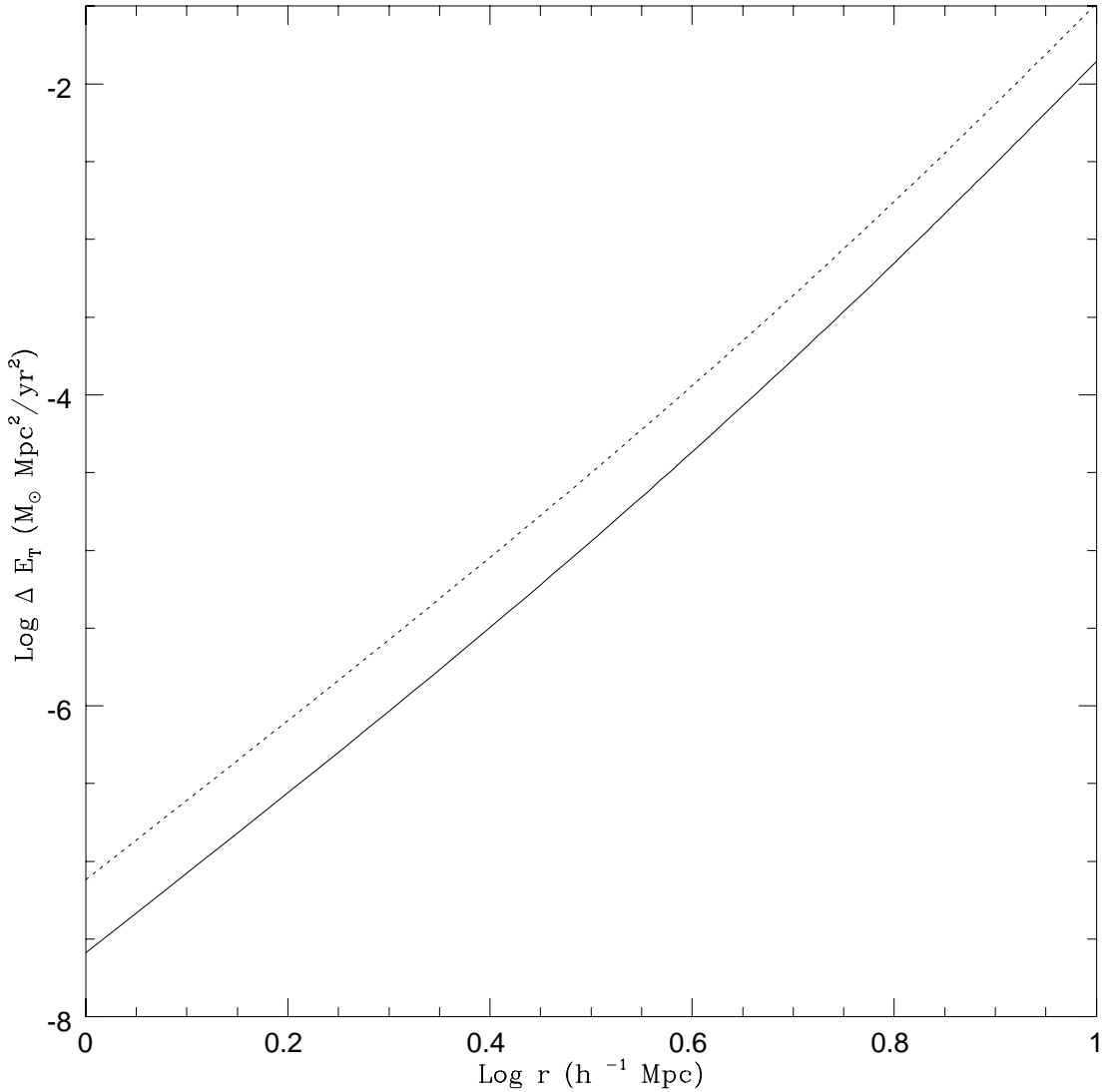


Fig. 2. Energy acquired during encounters of shells of matter infalling from a distance  $r$  from the centre of the proto-cluster. The dashed line represents  $\Delta E_T$  for the CDM spectrum, introduced in Section 2, smoothed on a scale  $R_f = 5h^{-1}$  Mpc and for  $\nu = 1.2$ . The solid line is the same but now  $\nu = 2$

where

$$N_{\text{pk}} = \frac{1}{(2\pi)^2} \frac{1}{R_*^3} G(\gamma, \gamma\nu) \exp(-\nu^2/2) \quad (35)$$

being  $G(\gamma, \gamma\nu)$  defined in Ref. 7 (equation (4.4)) together with  $R_*$  and  $\gamma$ , we obtain  $n_a \simeq 135 \text{Mpc}^{-3}$ . The average mass of the peaks with  $\nu \geq \nu_c$  is given by:

$$m_a = \frac{1}{n_a(\nu \geq \nu_c)} \int_{\nu_c}^{\infty} m_{\text{peak}} N_{\text{pk}}(\nu) d\nu \simeq 7 \times 10^8 M_{\odot} \quad (36)$$

where

$$m_{\text{peak}} = \frac{4\pi}{3} \rho_b R_*^3 \frac{2^{3/2}}{\gamma^3 + (0.9/\nu)^{3/2}} \quad (37)$$

(see Ref. 46). This mass satisfies both condition "aa)" and Silk & Stebbins<sup>39</sup> prescription for surviving clumps.

The fraction of this subpeaks satisfying the IA, and consequently satisfying condition "bb)", can be calculated using the conditional probability distribution  $f_{\text{pk}}(\mathbf{v}|\nu)$  giving the peculiar velocity around a peak of a gaussian density field having central height  $\nu$ :

$$f_{\text{pk}}(\mathbf{v}|\nu) = \frac{\frac{\alpha}{4\pi^2}}{\sqrt{\pi^3 \lambda_i}} \cdot e^{-\sum_{i=1}^3 \frac{[v_i - \nu \langle \nu v_i \rangle]^2}{\lambda_i}} \quad (38)$$

(see Ref. 37) ( $\langle \rangle$  denotes ensemble averages), where

$$\alpha = \frac{\sqrt{2}}{\pi} \text{erfc} \left[ \frac{\nu \langle \nu x \rangle}{\sqrt{\lambda x}} \right] \quad (39)$$

$\langle \nu x \rangle = \gamma$ , (Ref. 7)

$$\langle \nu v_i \rangle = -\frac{H_0 \Omega_0^{0.6} r_i}{r^3 \sigma_0} \int_0^r dx x^2 \xi(x) \quad (40)$$

$\xi(r)$  is the autocorrelation function and

$$x = -\frac{\nabla^2 \delta}{\sigma_2|_0} \quad (41)$$

is the central curvature of the peak.  $\lambda_1, \lambda_2, \lambda_3$  are three of the four eigenvalues of the covariance matrix  $M$  described in Antonuccio-Delogu & Colafrancesco<sup>37</sup>. These three eigenvalues represent the components of the peculiar velocity dispersions along directions parallel ( $\lambda_1$ ) and perpendicular ( $\lambda_2, \lambda_3$ ) with respect to the radial direction of a density peak. The fraction of peaks having  $v \geq v_{\text{esc}}$  can be obtained by means of the conditional probability distribution  $f_{\text{pk}}(v|\nu)$ :

$$F(v \geq v_{\text{esc}}) = \frac{\int_{|v| \geq v_{\text{esc}}}^{\infty} f_{\text{pk}}(v|\nu) d^3 v}{\int_0^{\infty} f_{\text{pk}}(v|\nu) d^3 v} \quad (42)$$

The fraction of peaks satisfying the condition  $F(v \geq v_{\text{esc}})$  can be easily calculated to be  $F(v \geq v_{\text{esc}}) = 0.00738$  for a Maxwellian velocity distribution,  $f(v) \propto \exp(-\frac{v^2}{2\sigma_v^2})$ , characterized by a uniform velocity dispersion  $\sigma_v^2$ . In the case of a top-hat perturbation of radius  $R_f = 1.5 h^{-1} \text{Mpc}$ ,  $F(v \geq v_{\text{esc}})$  can be as large as 0.3 for a typical velocity dispersion, and even larger for larger values of  $R_f$ .

Using the conditional probability distribution  $f_{\text{pk}}(\mathbf{v}|\nu)$ , in the case of a  $\nu = 1.2$  peak we get  $F(v \geq v_{\text{esc}}) \simeq 0.09 - 0.13$  within  $R_f = 5h^{-1}\text{Mpc}$ .

<sup>a</sup> In Fig. 1, we plot the spatial variation of  $F(v \geq v_{\text{esc}})$  for the CDM spectrum, introduced in Section 2, smoothed on a scale  $R_f = 5h^{-1}\text{Mpc}$  and for  $\nu = 1.2$ . In any case in the following, we'll make a conservative calculation using the lower estimates for  $F(v \geq v_{\text{esc}}) \simeq 0.09$ .

Finally, the total number of subpeaks verifying the above conditions "aa)", "bb)" is given by:

$$N_{\text{tot}} = \frac{4\pi}{3} r_i^3 \cdot n_a \cdot F(v \geq v_{\text{esc}}) \quad (43)$$

while the total energy,  $\Delta E_T$ , injected in the shell by the impulsive encounters with all high speed subpeaks is given by:

$$\Delta E_T = N_{\text{tot}} \cdot \Delta E \quad (44)$$

The energy for unit mass of a collapsing shell is a modified version of that given by Ref. 47 (equation( 19.9)) and can be written similarly to Ref. 48 in the form:

$$E = \frac{1}{2} \left( \frac{dr}{dt} \right)^2 - \frac{GM}{r} + \Delta E_T \quad (45)$$

where  $M$  is the mass of the shell of matter.

Integrating equation (45), using equations (25), (26) and remembering that  $\rho_i = \rho_{ci}(1 + \bar{\delta})$  where  $\rho_{ci} = \frac{3H_i^2}{8\pi G}$ , with  $\rho_{ci}$  and  $H_i$  respectively the critical mass density and the Hubble constant at the time  $t_i$ , the time of collapse is given by:

$$t_c = 2 \int_0^{a_{\text{max}}} \frac{da}{\sqrt{H_i^2 \left[ \frac{1+\bar{\delta}}{a} - \frac{1+\bar{\delta}}{a_{\text{max}}} \right] - \frac{4G}{H_i^2(1+\bar{\delta})r_i^5} \Delta E_T}} \quad (46)$$

Integrating analytically equation (46), we find the solution:

$$t_c/2 \simeq \frac{\pi}{H_i} \frac{1}{\left( \bar{\delta} + \frac{4G}{H_i^4 r_i^5} \Delta E_T \right)^{3/2}} \quad (47)$$

having assumed  $\bar{\delta} \ll 1$ . In the case  $\Delta E_T = 0$  the solution of this equation is that given In Ref. 2:

$$t_{c0}/2 \simeq \frac{\pi}{H_i} \frac{1}{\bar{\delta}^{3/2}} \quad (48)$$

---

<sup>a</sup>It is important to note that the use of the peak formalism is not fundamental for what concerns the results of this paper. Similar results are obtained even using a top-hat perturbation for which, has previously remarked,  $F(v \geq v_{\text{esc}})$  can be as large as 0.3.

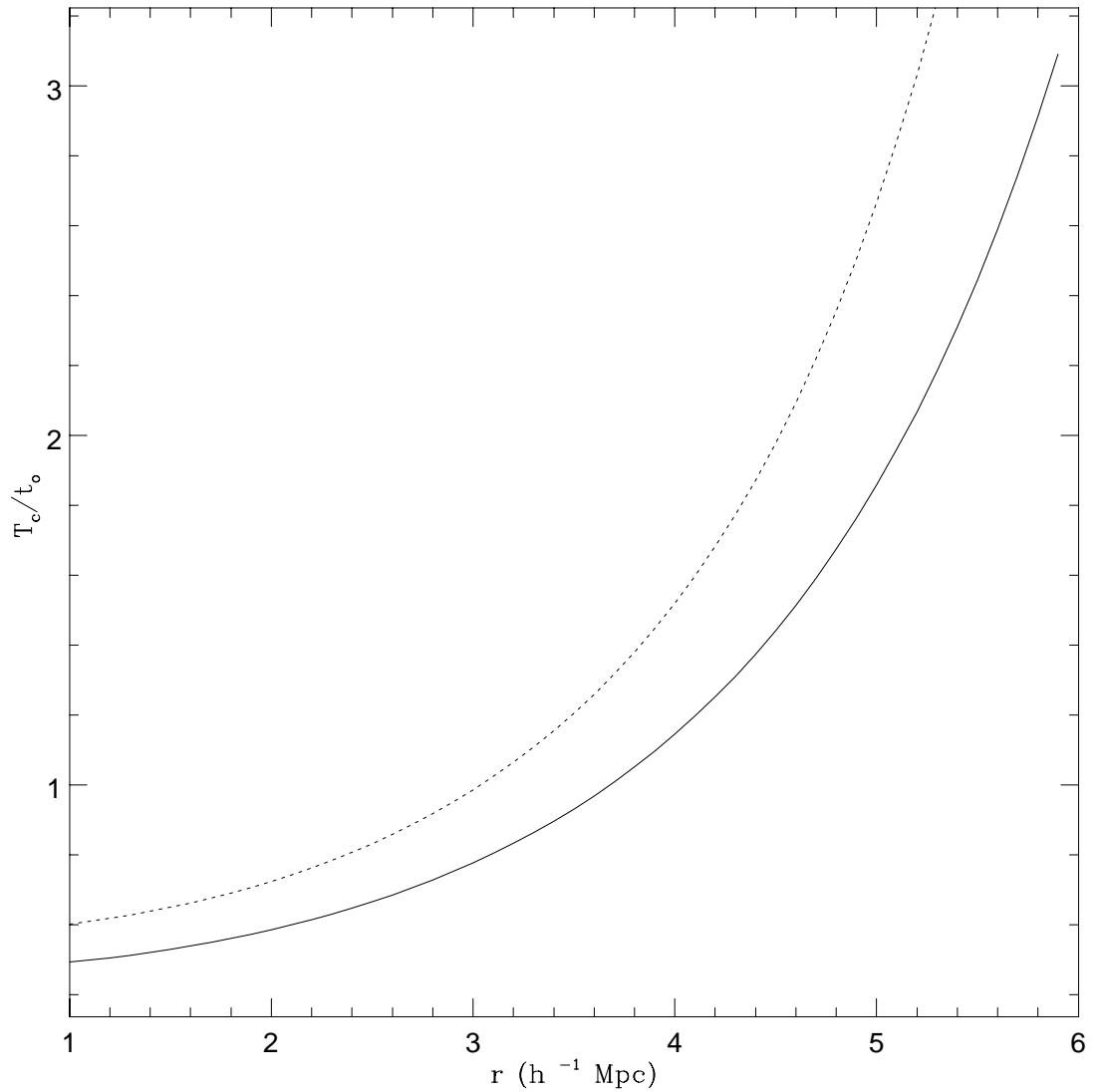


Fig. 3. The time of collapse of a shell of matter around a peak having  $\nu = 1.2$  in a CDM model taking account of the effect of the unbound high velocity clumps (solid line) and for the Gunn & Gott<sup>2</sup> model (dashed line).  $t_0$  is Hubble time.

### 3. Results and discussion

The results found by means of the model introduced in the previous section are shown in the Fig. 1-5.

As previously reported, Fig. 1 shows the spatial variation of  $F(v \geq v_{\text{esc}})$  for the CDM spectrum, introduced in Section 2, smoothed on a scale  $R_f = 5h^{-1}$  Mpc and for  $\nu = 1.2$ . The fraction of clumps with  $v \geq v_{\text{esc}}$  within  $R_f = 5h^{-1}$  Mpc is  $F(v \geq v_{\text{esc}}) \simeq 0.09 - 0.13$ , and increases with increasing radius. This behavior is due to the fact that the potential of the structure becomes shallower going towards its outskirts, and consequently  $v_{\text{esc}}$  is substantially lower. In Fig. 2 we show the total energy injected in the shell, because of the impulsive encounters of collapsing shells with the high speed clumps, in function of the initial radius of the shell. The dashed line represents  $\Delta E_T$  for a CDM model with spectrum given by equation (33) for  $\nu = 1.2$ . As shown, shells collapsing from larger distances from the centre of the cluster acquire more energy. This is due to two different reasons: firstly the energy,  $\Delta E$ , acquired in an encounter with a single clump increases with increasing turn-around radius of the shell of matter. Secondly,  $\Delta E_T$ , is proportional to the number of unbound clumps that increases with radius (see equation (43)) and then a shell falling from a larger distance encounters more unbound clumps. The solid line represents  $\Delta E_T$  for  $\nu = 2$ . The value of  $\Delta E_T$  is smaller with respect to the previous case. The reason is due to the fact that the fraction of the unbound peaks decreases for higher  $\nu$  peaks because the potential of these protostructures is deeper and hence the value of  $v_{\text{esc}}$  is systematically higher.

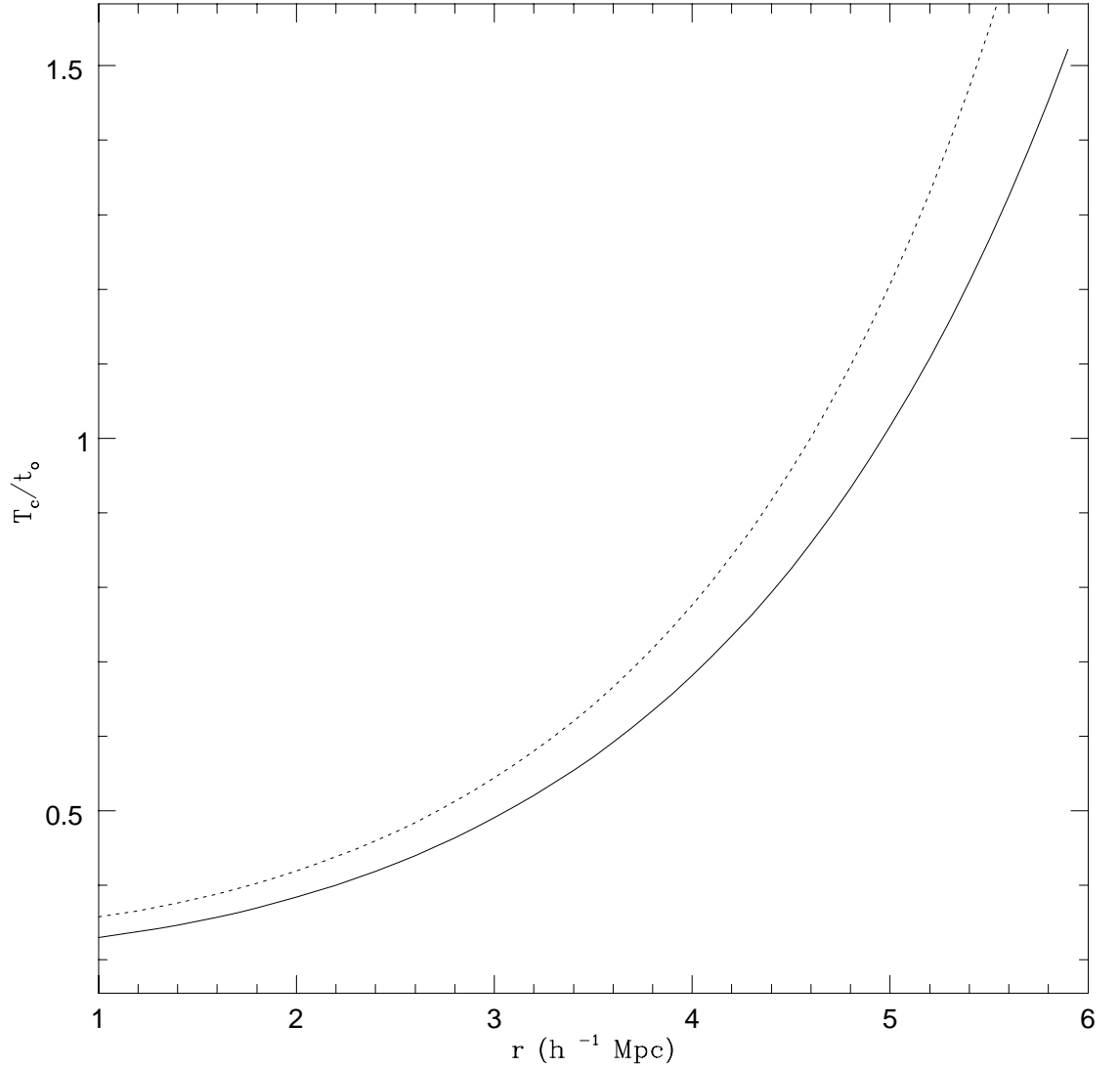
In Fig. 3 we show the collapse time versus the distance from the centre of the cluster. The figure plots the collapse time from  $1 h^{-1}$  Mpc on, because of the limits of the IA, stressed by Ref. 42, in the central part of the cluster. The solid line represents,  $t_c$ , for  $\nu = 1.2$  and taking account of the unbound clumps effect, while the dashed line is the collapse time,  $t_{c0}$ , given by the model in Ref. 2. This figure shows that the collapse time is accelerated, with respect to the model in ref. 2, because of the energy acquired by the shells during encounters with unbound clumps. In Fig. 4 we show  $t_c$ , for  $\nu = 2$ . As in the previous figure the solid line represents  $t_c$  taking account of the unbound clumps effect, while the dashed line represents  $t_{c0}$  given by the model in Ref. 2. Comparing Fig. 3 and Fig. 4 we see that the effect of the unbound peaks on the acceleration of the collapse time is larger in the case  $\nu = 1.2$ . This is in agreement to what observed for  $\Delta E_T$ .

Finally, in Fig. 5 we make a comparison between the acceleration in collapse time due to unbound clumps to the slowing down effect produced by the gravitational interaction of the quadrupole moment of the system with the tidal field of the matter of the neighboring proto-clusters, described in Ref. 3.

As shown in Fig. 5, the magnitude of the two effects is comparable at  $1h^{-1}$  Mpc, but the accelerating effect produced by the high speed clumps decreases with increasing distance from the cluster centre, with respect to the slowing down effect produced by the tidal field.

The mechanism considered in this paper is different from that described in Ref. 3 for two reasons:

- the delay of the collapse produced by unbound clumps is due to encounters

Fig. 4. Same as Fig. 3 but now  $\nu = 2$ 

of infalling shells of matter and unbound clumps. The effect described in Ref. 3 is produced by tidal interaction of the matter of a given protocluster with that of the neighboring ones;

- the substructure responsible for collapse delay in this paper is that contained inside the infalling shell while in Ref. 3 it is external to the shell.

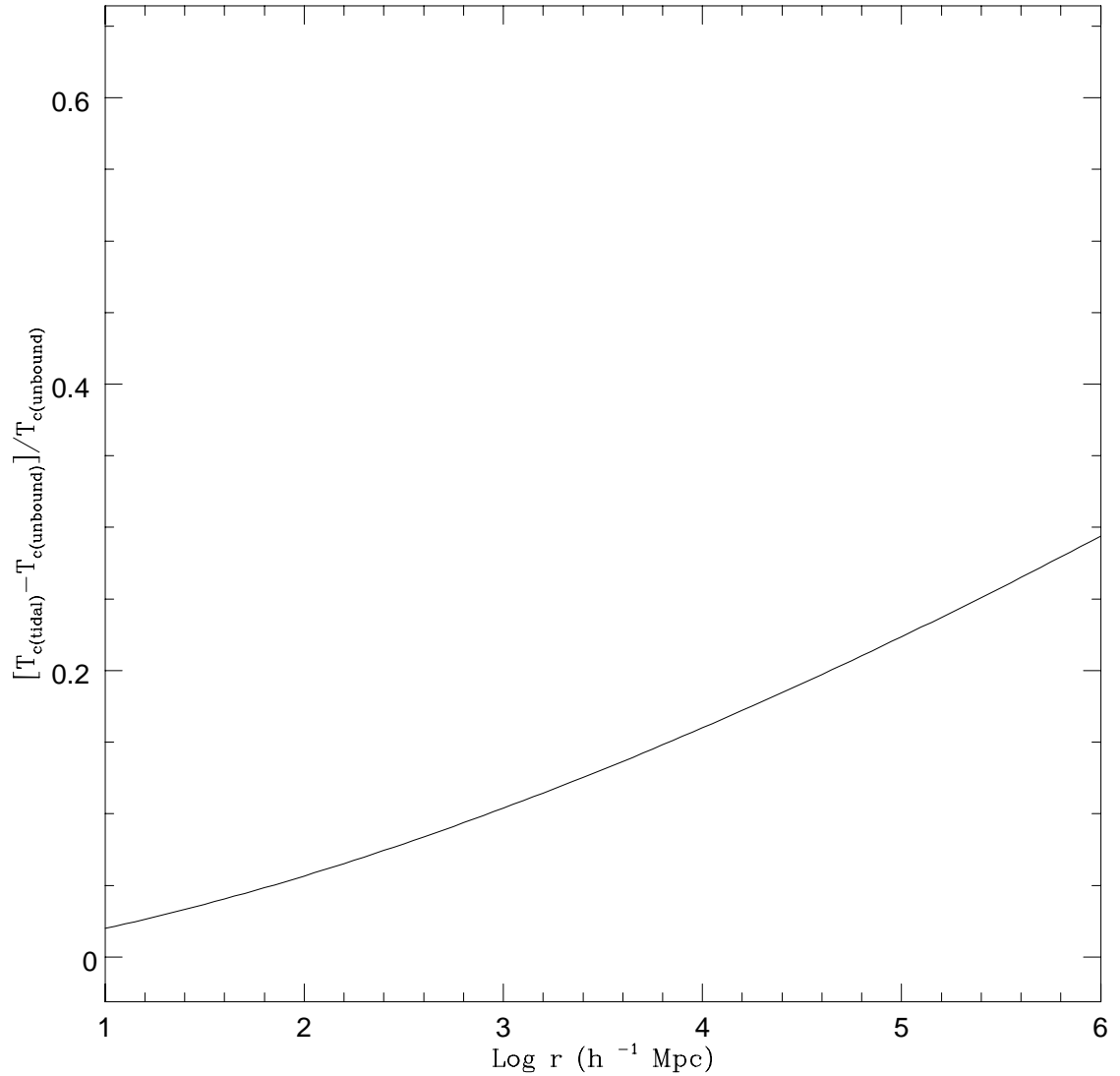


Fig. 5. Comparison of the collapse time  $T_{c(\text{unbound})}$ , obtained taking account unbound high velocity clumps, with  $T_{c(\text{tidal})}$ , obtained taking account of the tidal interaction of the protocluster with the neighboring ones. In this case  $\nu = 2$

The two effects have a different physical origin, and act in the opposite direction: unbound clumps accelerate the collapse, the effect of the tidal field is to delay the shell collapse. It is obvious that during the infall of a shell both effects are

present with the final result that at small radii ( $\simeq 1h^{-1}\text{Mpc}$ ) they counterbalance while at larger radii tidal field is dominant producing a slowing down of the shell collapse. We want to stress that the idea that high velocity clumps can influence the collapse and secondary infall of matter in protoclusters was introduced (but not developed) in a paper by Antonuccio & Colafrancesco<sup>37</sup>. In the conclusion of that paper, regarding the velocity correlation tensor and unbound substructure around density peaks, they noted that high velocity clumps can exchange momentum with the collapsing or infalling clumps and generate a drag force onto the collapsing material with a consequent delay of the collapse. According to their paper the drag force is due to dynamical friction. Unfortunately this last considerations are not quite right because:

1) the effects of the high velocity clumps on the collapse shell of matter cannot be calculated using the dynamical friction approximation since a necessary condition to apply this last is that the encounter of two systems is characterized by  $V \simeq v_{\text{tip}}$  (where  $v_{\text{tip}}$  is the internal velocity of the system) (see Ref. 44). To be more precise, according to Ref. 49, a body of mass  $M$  moving through a homogeneous and infinite distribution of bodies of mass  $m$ , that we call field particles, is subject to the deceleration:

$$\frac{d\mathbf{v}_M}{dt} = -16\pi^2 \ln \Lambda G^2 m(M+m) \frac{\int_0^{v_M} f(v_m) v_m^2 dv_m}{v_M^3} \mathbf{v}_M \quad (49)$$

where  $\ln \Lambda$  is the Coulomb logarithm and  $f(v_m)$  is the phase-space number density field particles. As clearly stated by equation (49) only field particles moving slower than  $M$  contribute to the force. In our case, the role of the field particles is played by the high speed clumps that have speeds much larger than those characterizing the motion of the shell particles (when IA is satisfied) or at least a bit larger.

2) The effects of the high velocity clumps is to accelerate the shell collapse and not to delay it.

We note that the erroneous conclusion of Antonuccio & Colafrancesco<sup>37</sup> paper is not connected with their analysis of the conditional probability distribution  $f_{\text{pk}}(\mathbf{v}|\nu)$  developed in the paper, that we used to calculate the number of subpeaks satisfying the IA. The erroneous conclusion is due to the way they thought to calculate the interaction between the high velocity clumps and the infalling shells.

#### 4. Conclusions

In this paper we have studied the role of unbound high velocity clumps on the collapse of density peaks in a SCDM model ( $\Omega_0 = 1$ ,  $h = 0.5$ ,  $n = 1$ ). We have shown that:

- 1) the encounters of collapsing shells with unbound clumps produce an acceleration in the collapse of density peaks. The effect is larger for peaks having a lower value of  $\nu$  (see Fig. 2  $\div$  3).
- 2) A comparison between the collapse acceleration due to encounters of shells with

unbound clumps and the slowing down effect produced by tidal interaction between a protocluster and the neighboring ones (see Ref. 3) has shown that these two effects act in opposite direction, namely the first accelerate the shell collapse, while the second delay the protocluster collapse, especially in its outskirts. The magnitude of the two effects is comparable at  $1h^{-1}\text{Mpc}$  but the effect of the tidal field dominates at larger radii.

3) The acceleration in the collapse is due to the additive action of several high speed clumps with the matter of the infalling shells.

### Acknowledgments

We are grateful to E. Spedicato, E. Recami, G. Mamon and O. Gnedin for stimulating discussions during the period in which this work was performed and whose comments and suggestions helped us to improve the quality of this work. A. Del Popolo and E.Nihal Ercan would like to thank Boğaziçi University Research Foundation for the financial support through the project code 01B304.

### References

1. Aguilar L.A., White S.D.M., 1985, *ApJ*, 295, 374
2. Gunn J.E., Gott J.R., 1972, *ApJ*, 176, 1 (GG)
3. Del Popolo A., Gambera M., 1998, *A&A*, 337, 96 (DG)
4. Guth A.H., Pi S.Y., 1982, *Phys.Rev.Lett.*, 49, 1110
5. Hawking S.W., 1982, *Phys.Lett B*, 115, 295
6. Starobinsky A.A., 1982, *Phys.Lett. B*, 117, 175
7. Bardeen J.M., Bond J.R., Kaiser N., Szalay A.S., 1986, *ApJ*, 304, 15 (BBKS)
8. Kaiser N., 1984, *ApJ*, 284, L9
9. Filmore J.A., Goldreich P., 1984, *ApJ*, 281, 1
10. Bertschinger E., 1985, *ApJS* 58, 39
11. Hoffman Y., Shaham J., 1985, *ApJ*, 297, 16
12. Quinn P.J., Salmon J.K., Zurek W.H., 1986, *Nature*, 322, 329
13. West M.J., Dekel A., Oemler A., 1987, *ApJ*, 316, 1
14. Ryden B.S., Gunn J.E., 1987, *ApJ* 318, 15
15. Ryden B.S., 1988, *ApJ*, 329, 589
16. Hoffman Y., 1988, *ApJ*, 328, 489
17. Efstathiou G., Frenk C.S., White S.D.M., Davis M., 1988, *MNRAS*, 235, 715
18. White S.D.M., Zaritsky D., 1992, *ApJ*, 394, 1
19. Evrard, A.E., Mohr, J.J., Fabricant, D.G., Geller, M.J., 1993, *ApJ*, 419, L9
20. Crone M.M., Evrard A.E., Richstone D.O., 1994, *ApJ*, 434, 402
21. Navarro J.F., Frenk C.S., White S.D.M., 1995, *MNRAS*, 275, 720
22. Navarro J.F., Frenk C.S., White S.D.M., 1996, *ApJ*, 462, 563
23. Navarro J.F., Frenk C.S., White S.D.M., 1997, *ApJ*, 490, 493
24. Avila-Reese V., Firmani C., Hernandez X., 1997, *preprint Sissa astro-ph/9710201*
25. Hoyle F., Narlikar, J.V., 1966, *Proc. Roy. Soc. A*290,177
26. Gott J.R., 1975, *ApJ*, 201, 296
27. Gunn J.E., 1977, *ApJ*, 218, 592
28. Regös E., Geller M.J., 1989, *AJ*, 98, 755

29. Briel U.G., Henry J.P., Schwarz R.A., et al.
30. Del Popolo A., Gambera M., Spedicato E., Recami E., 2000a, *A&A*, 353, 427
31. Del Popolo A., Gambera M., 1999, *A&A*, 344, 17
32. Del Popolo A., Takahashi Y., Kiuchi H., Gambera M., 1999, *A&A*, 348, 667
33. Del Popolo A., Gambera M., 2000b, *A&A*, 357, 809
34. Beers T.C., Geller M.J., 1983, *ApJ*, 274, 491
35. Jones C., Forman W., 1984, *ApJ*, 276, 38
36. Dressler A., Shectman S.A., 1988, *AJ*, 95, 985
37. Antonuccio-Delogu V., Colafrancesco S., 1995, *preprint Sissa astro-ph/9507005*
38. Liddle A.R., Lyth D.H., 1993, *Phys. Rep.*, 231, n 1, 2
39. Silk J., Stebbins A., 1993, *ApJ*, 411, 439
40. Rees M.J., 1986, *MNRAS*, 218, 25p
41. Henon, M., 1964, *Ann. d'ap.*, 27, 83
42. Gnedin, O.Y., Ostriker J.P., 1999, *astro-ph/9902326*
43. Del Popolo A., Gambera M., 1997, *A&A*, 321, 691
44. Binney J., Tremaine S., 1987, *Galactic Dynamics*, in *Princeton Series in Astrophysics*, Princeton University Press.
45. Antonuccio-Delogu V., Colafrancesco S., 1994, *ApJ*, 427, 72
46. Peacock J.A., Heavens A.F., 1990, *MNRAS*, 243, 133
47. Peebles P.J.E., 1980, *The large scale structure of the Universe*, Princeton university press
48. Peebles P.J.E., 1993, *Principles of Physical Cosmology*, Princeton University Press
49. Chandrasekar S., 1943, *ApJ*, 97, 255